

Supporting Information

Barium-based scintillating MOFs for X-ray dosage detection with intrinsic energy resolution via luminescent multidentate naphthalenedisulfonate moieties

Jian Lu,^{abc} Juan Gao,^{ab} Wen-Fei Wang,^{ab} Bao-Yi Li,^{ab} Pei-Xin Li,^a Fa-Kun Zheng^{*ab} and Guo-Cong Guo^{*ab}

^a *State Key Laboratory of Structural Chemistry, Fujian Institute of Research on the Structure of Matter, Chinese Academy of Sciences, Fuzhou, Fujian 350002, P. R. China. E-mail: zfk@fjirsm.ac.cn; Fax: (+86)591-63173068; Tel: +86-591-63173889.*

^b *Fujian Science & Technology Innovation Laboratory for Optoelectronic Information of China, Fuzhou, Fujian 350108, P. R. China.*

^c *State Key Laboratory of Quality Research in Chinese Medicine, Institute of Chinese Medical Sciences, University of Macau, Taipa, Macau, P.R. China.*

Experimental section

All of the chemicals were purchased from commercial sources and were used without further purification. Organic ligands (disodium 1,5-naphthalenedisulfonate (1,5-Na₂nds), disodium 1,6-naphthalenedisulfonate (1,6-Na₂nds) and disodium 2,7-naphthalenedisulfonate (2,7-Na₂nds)) and metal ion salts BaCl₂·2H₂O were purchased from Adamas-beta® chemical industrial company. *N,N*-Dimethylformamide (DMF, 99.9%) and ethanol were from Sinopharm Chemical Reagent Co., Ltd. Ultrapure water was self-prepared and used throughout all experiments.

Synthesis of Compounds 1–3

Compounds **1–3** were synthesized through solvothermal reactions ([Scheme S1](#)).

[Ba(1,5-nds)H₂O]_n **1** An aqueous solution (2 mL) of BaCl₂·2H₂O (73.29 mg, 0.3 mmol) was added to a DMF/EtOH solution (8 mL, V:V 1:1) of 1,5-Na₂nds (83.07 mg, 0.25 mmol). The resultant solution was sealed in a 25 mL Teflon-lined stainless vessel under autogenous pressure, slowly heated to 100 °C in 6 hrs, kept at 100 °C for 72 hrs, and then slowly cooled to 30 °C in 12 hrs. Colorless transparent prism crystals of **1** were formed, then collected and washed with methanol for several times, finally obtained in 76% yield after being dried under vacuum oven (based on 1,5-Na₂nds). FT-IR (KBr pellet, cm⁻¹): 3572 m, 3501 m, 3098 w, 1643 m, 1602 w, 1575 w, 1503 m, 1400 m, 1354 m, 1253 m, 1206 s, 1153 w, 1049 s, 924 w, 792 s, 771 s, 662 m, 606 s, 569 w, 525 w.

[Ba(1,6-nds)H₂O]_n **2** The reaction procedure of compound **2** is similar to that of compound **1**, except that ligand 1,6-Na₂nds (83.07 mg, 0.25 mmol) was in place of 1,5-Na₂nds. The colorless transparent prism crystals of compound **2** were obtained in 54% yield (based on 1,6-Na₂nds). FT-IR (KBr pellet, cm⁻¹): 3560 m, 3442 m, 3109 w, 1656 m, 1596 m, 1502 m, 1231 s, 1181 s, 1108 s, 1077 w, 1051 m, 1033 w, 972 m, 886 m, 827 m, 788 m, 749 m, 702 m, 673 s, 620 m, 584 m, 551 w, 510 m.

[Ba(2,7-nds)(H₂O)₂]_n **3** The reaction procedure of compound **3** is also very similar to that of compound **1**, except that ligand 2,7-Na₂nds (83.07 mg, 0.25 mmol) was in place of 1,5-Na₂nds. The colorless transparent prism crystals of compound **3** were obtained in 61% yield (based on 2,7-

Na₂nds). FT-IR (KBr pellet, cm⁻¹): 3557 m, 3439 m, 3078 w, 1640 m, 1504 w, 1413 w, 1322 m, 1250 s, 1271 m, 1218 s, 1175 s, 1110 s, 1039 s, 946 m, 926 m, 845 m, 708 s, 671 m, 631 m, 605 m, 574 m.

X-ray crystallography

Single-crystal X-ray diffractions of compounds **1–3** were performed by a Rigaku PILATUS CCD diffractometer equipped with graphite-monochromated Mo K_{α} radiation ($\lambda = 0.71073 \text{ \AA}$) at 293 K. The intensity data sets were collected using a ω -scan technique and reduced using *CrysAlisPro* software.¹ The structures were solved by direct methods, and the subsequent successive difference Fourier syntheses yielded other nonhydrogen atoms. All atoms except hydrogen atoms were performed through the anisotropic refinement. The hydrogen atoms were calculated in the idealized positions and refined with riding coordinates on their parent atoms. The final structures were refined using a full-matrix least-squares refinement on F^2 with the *Olex2 1.2* program.^{2–4} Pertinent crystal data and structure refinements are summarized in **Table S1**. The selected bond lengths and angles are listed in **Tables S2**. Related hydrogen bond information is given in **Table S3**.

Physical characterization

Powdered X-ray diffraction patterns (PXRD) were recorded with a Miniflex 600 at 40 kV, 40 mA for Cu- K_{α} with a scan speed of 0.10s per step and a step size of 0.02°, the data were collected within 2θ range of 5–65°. The Mercury Version 2020.1 software (https://www.ccdc.cam.ac.uk/support-and-resources/Downloads#8a6058f8-d386-e511-91c5-005056868fc8_ce657cfc-4cbd-e611-807a-005056868fc8_collapse) was utilized to achieve simulated PXRD patterns dependent on the X-ray crystallographic structure. Fourier transform infrared spectra (FT-IR) were measured with KBr slices from 4000 to 400 cm⁻¹ using a VERTEX 70 infrared spectrum radiometer. Solid state UV-visible diffuse reflectance spectra were taken by PerkinElmer Lambda 365, while the absorption spectra were conducted under dilute water solution state by Shimadzu UV2600 spectrophotometer. Thermogravimetric analysis (TGA) was

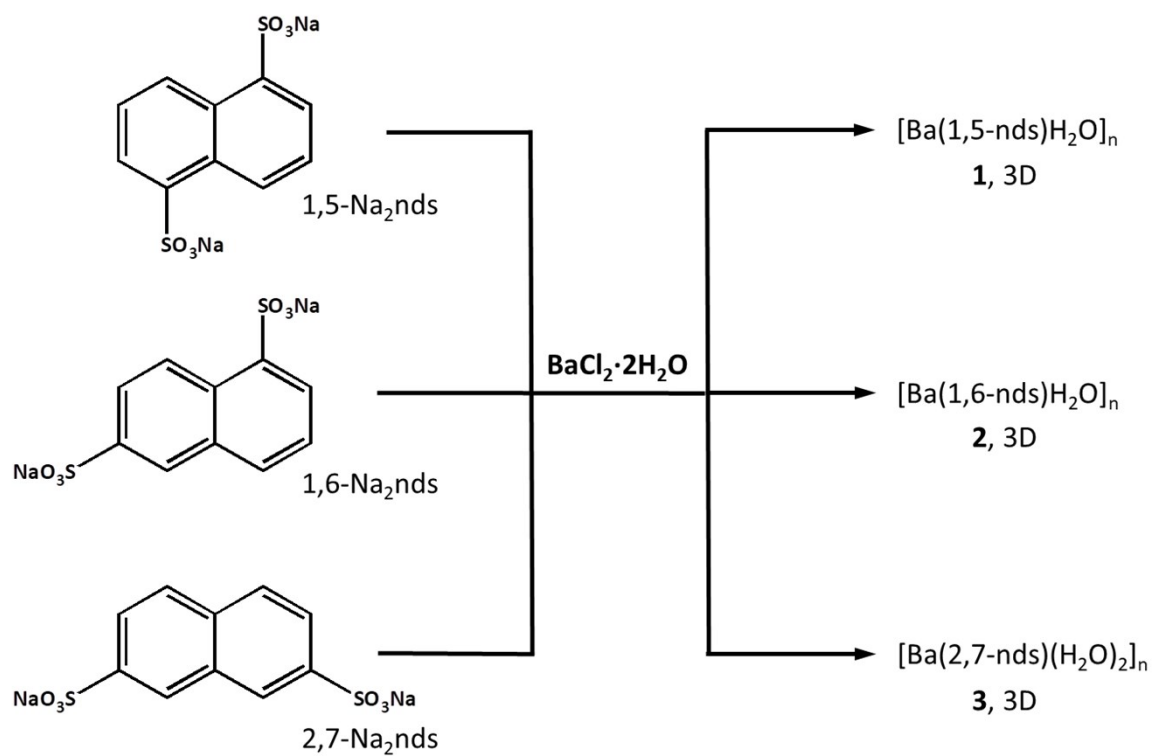
measured using a METTLER TOLEDO system at a heating rate of 10 K min^{-1} under nitrogen atmosphere. The photoluminescence spectra were recorded on an Edinburgh FLS920 phosphorimeter using a 450W Xenon lamp as excitation source.

Scintillating measurements

The X-ray stimulated luminescence (XSL) spectra were recorded on our self-built scintillating measurement equipment.⁵ The whole backbone of the X-ray stimulated Fluorescence Spectrometer was from FLS920 Spectrometer, except that the excitation Xe lamp is replaced by a highly purified tungsten target (Moxtek® MAGPRO X-ray sources: <http://moxtek.com/xray-product/60kv-70kv-12w-magpro-x-ray-source/>). The used photomultiplier tube in detecting the X-ray induced photons is HAMAMATSU R928.

Calculation of electronic structures and density of states (DOS)

The calculation models were built directly from X-ray crystallographic data to calculate the energy band structures. Calculations of the electronic structures and DOS were carried out by the CASTEP code based on DFT with GGA-PBE functional in the Materials Studio v7.0 software package.⁶ Energy cutoff was determined to be 750 eV for compounds **1–3**, and numerical integration of Brillouin zone was employed by monkhorst-Pack *K*-point of $3 * 1 * 4$ for compound **1**, $2 * 2 * 1$ for compound **2** and $2 * 1 * 5$ for compound **3**.



Scheme S1 The synthetic route of compounds 1-3.

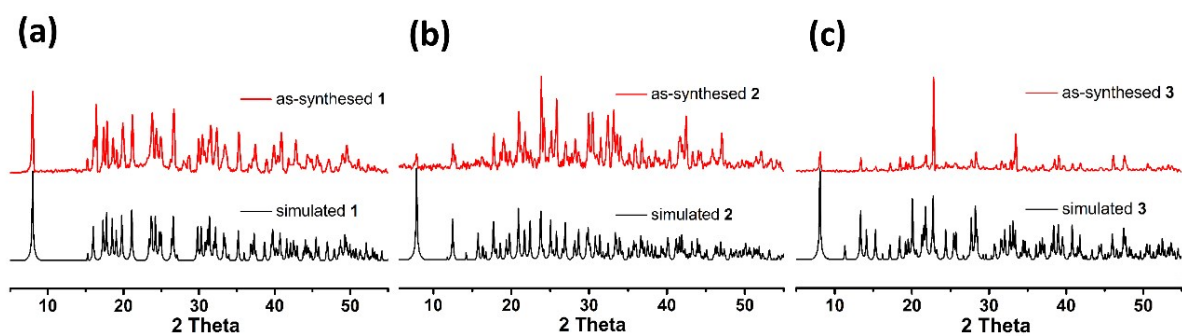


Fig. S1 The PXRD patterns of compounds (a) 1, (b) 2 and (c) 3.

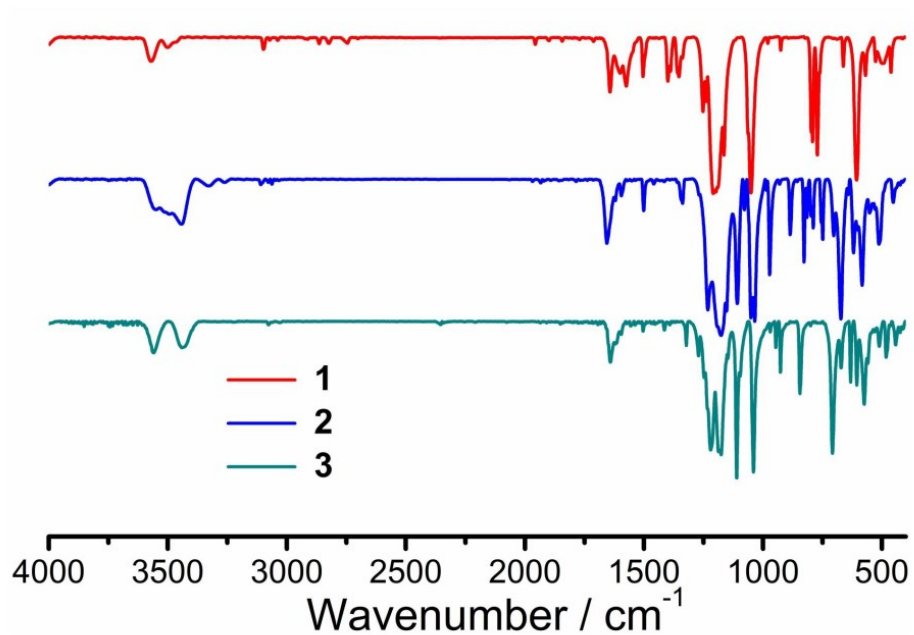


Fig. S2 The FT-IR curves of compounds **1-3** recorded using KBr pellet.

Analysis: The specific features observed at 1206, 1049 cm⁻¹ of **1**, 1181, 1108 cm⁻¹ of **2** and 1175, 1110, 1039 cm⁻¹ of **3** suggest the strong coordination effects of the corresponding ligand to the metal Ba(II) ions.⁷

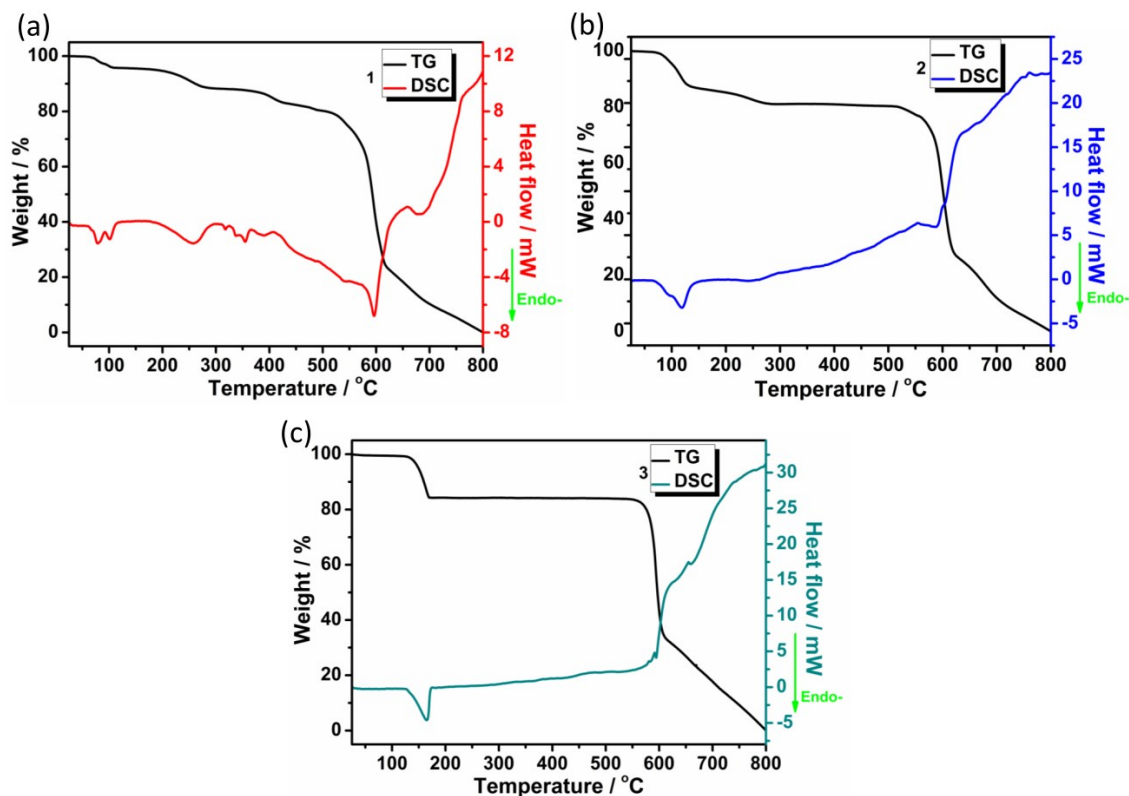


Fig. S3 The TG-DSC curves of compounds (a) 1, (b) 2 and (c) 3.

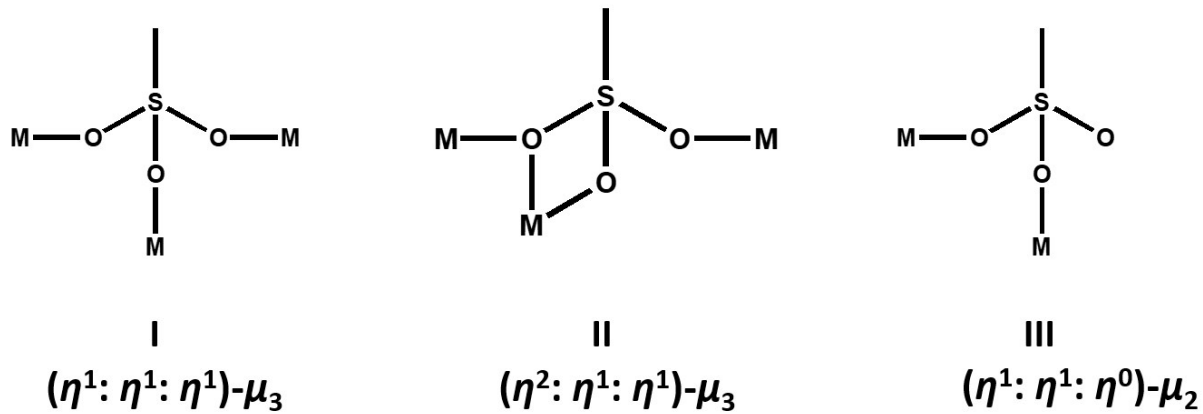


Fig. S4 The various coordination modes of sulfonate groups in ligands nds^{2-} .

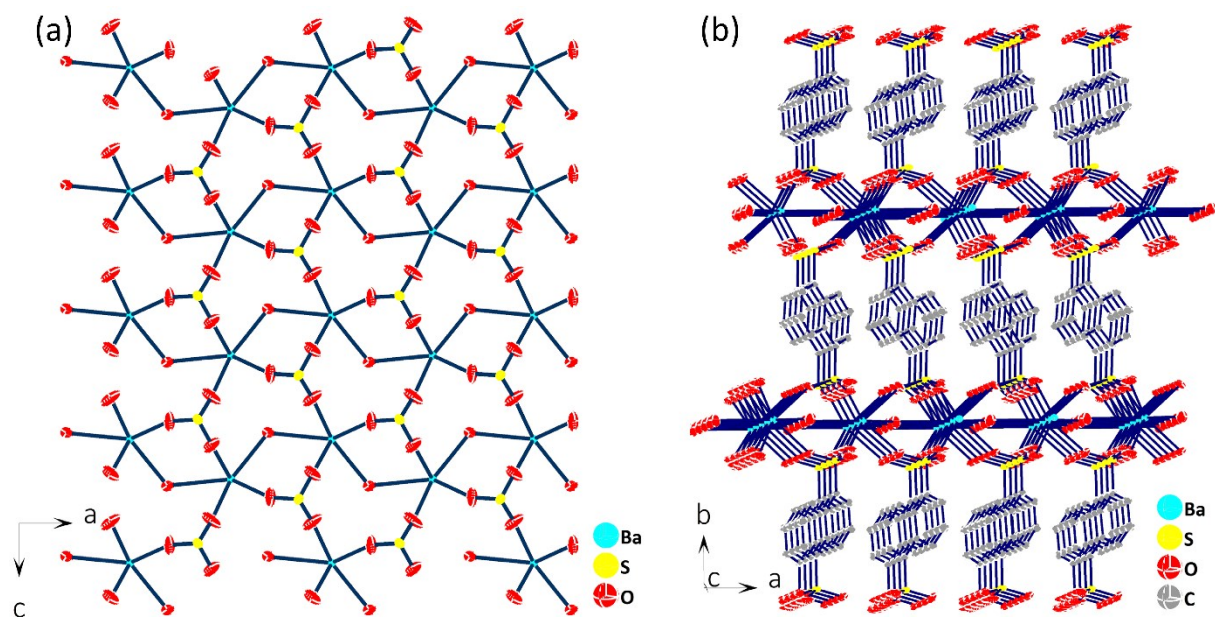


Fig. S5 For 1: (a) the constructed 2D plane parallel to the ac plane and (b) the 3D open frameworks viewing from $[0 0 1]$ direction.

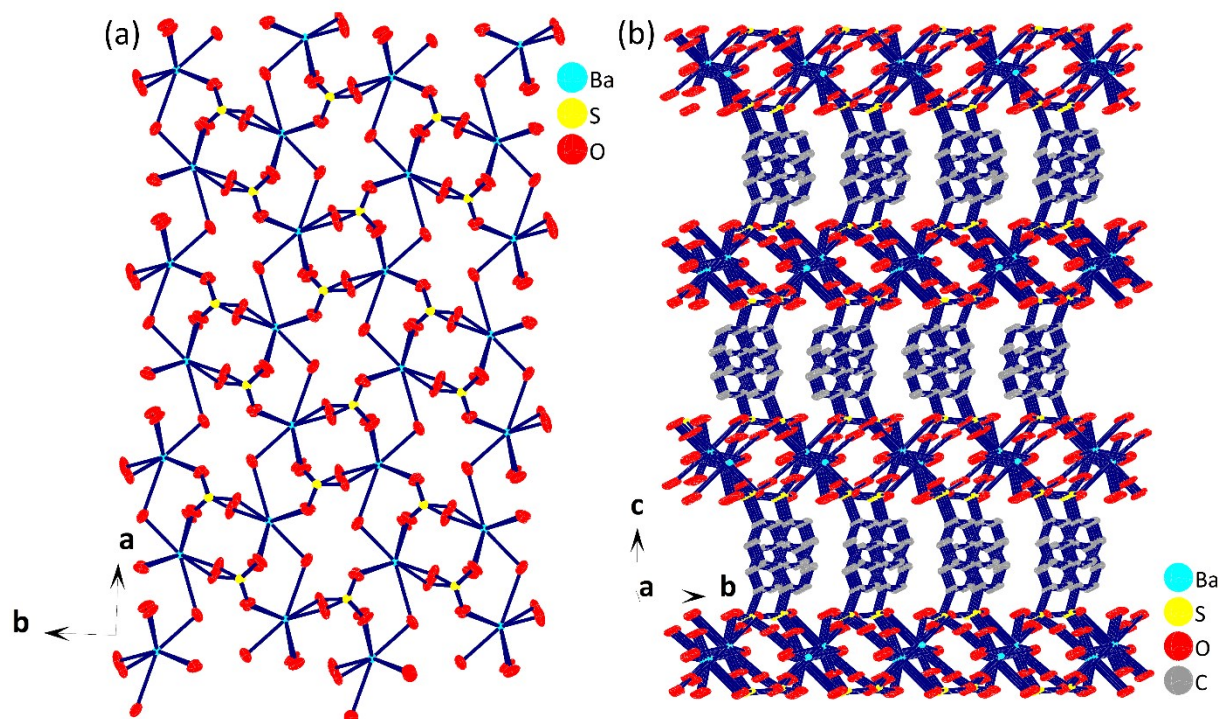


Fig. S6 For 2: (a) the constructed 2D plane parallel to the ab plane and (b) the 3D open frameworks viewing from $[1 0 0]$ direction.

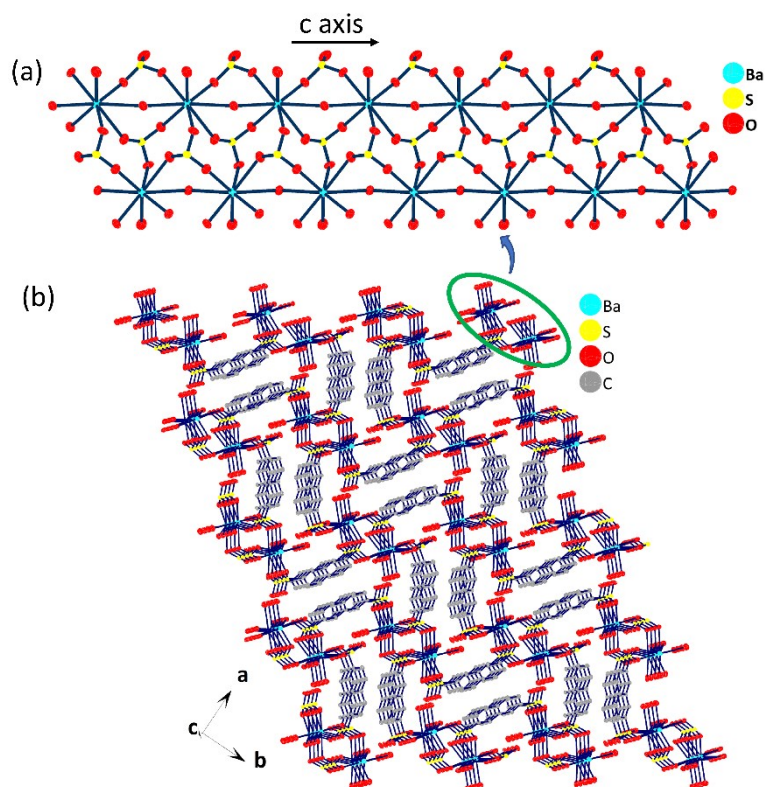


Fig. S7 For **3**: (a) the dinuclear Ba-S-O rod along the c axis and (b) the 3D open frameworks viewing from $[0\ 0\ 1]$ direction.

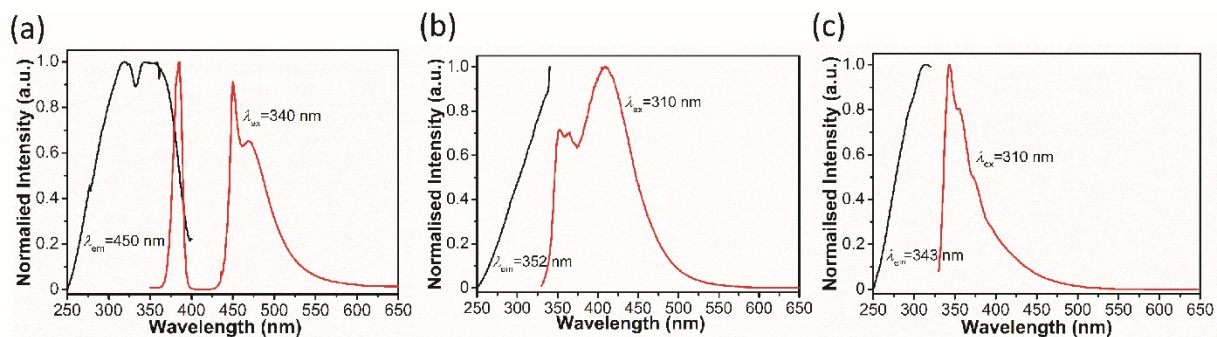


Fig. S8 The normalized solid-state steady excitation (black line) and emission (red line) spectra of compound (a) **1**, (b) **2** and (c) **3**.

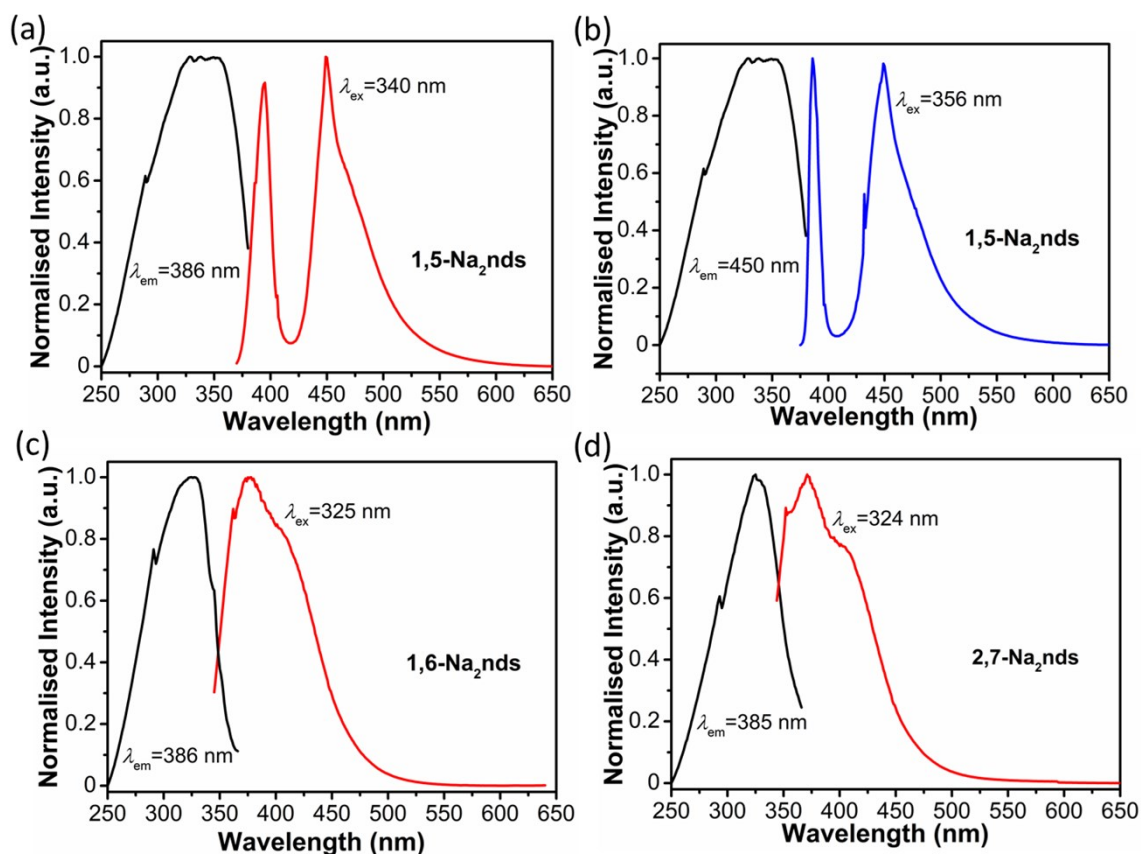


Fig. S9 The normalized solid-state steady excitation (black line) and emission (red/blue line) spectra of free ligand (a) and (b) 1,5- Na_2nds , (c) 1,6- Na_2nds and (d) 2,7- Na_2nds .

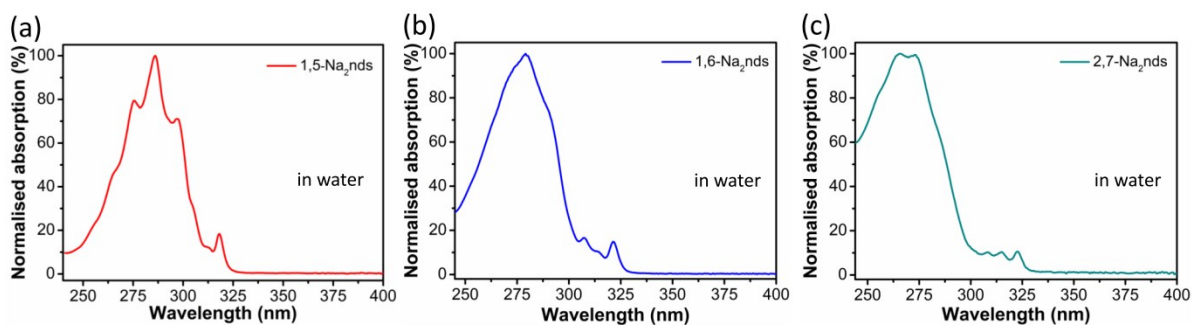


Fig. S10 The normalized UV-Vis absorption spectra of ligand (a) 1,5- Na_2nds , (b) 1,6- Na_2nds and (c) 2,7- Na_2nds in dilute water solvent.

Analysis:

The minor absorption peak around 320 nm for the free ligands 1,5- Na_2nds , 1,6- Na_2nds and 2,7- Na_2nds could be attributed to the $n \rightarrow \pi^*$ charge transfer, also called *R* band absorption, in which the lone pair electrons from the O atom of the sulfonate group can easily get excited to leap into the π^* orbital of the naphthalene nucleus.

The strong absorption peak ranging from 250 – 300 for the free ligands 1,5-Na₂nds, 1,6-Na₂nds and 2,7- Na₂nds could be attributed to the $\pi \rightarrow \pi^*$ charge transfer, typical *B* band absorption for the π -electron rich systematic naphthalene motif.⁸

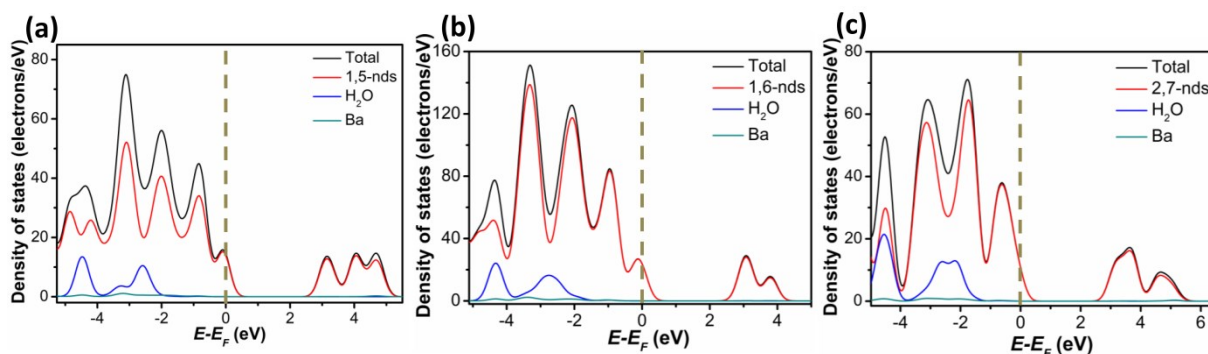


Fig. S11 Density of state profiles of compound (a) **1**, (b) **2** and (c) **3**.

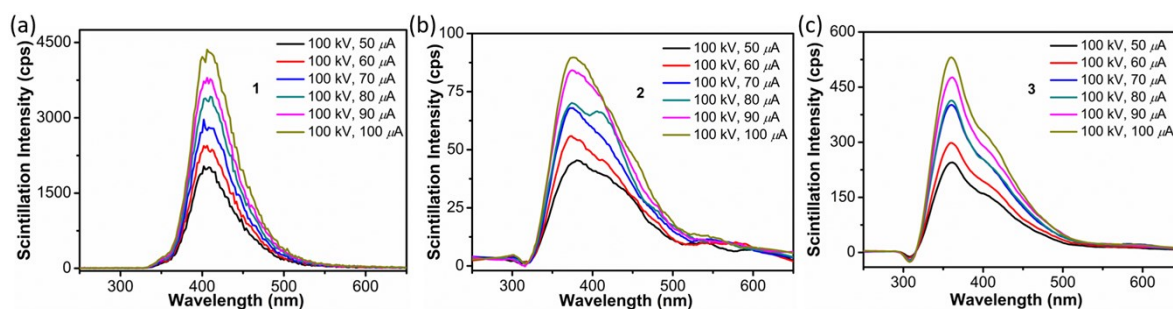


Fig. S12 The X-ray stimulated luminescent (XSL) spectra of compound (a) **1**, (b) **2** and (c) **3** triggered by tungsten target with high purity under the working conditions via our self-built X-ray scintillation instrument with fixed tube voltage at 100 kV and tube current varied from 50 to 100 μ A.

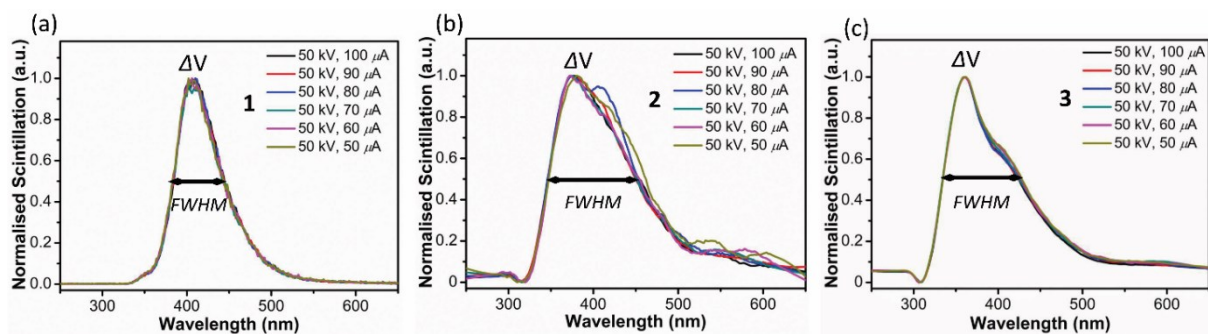


Fig. 13 The normalized X-ray scintillating spectra for energy resolution clarification: (a) compound **1**, (b) compound **2** and (c) compound **3**, respectively.

Table S1. Crystallographic data for compounds **1-3**.

Crystal data	1	2	3
CCDC number	2024552	2024553	2024554
Empirical formula	C ₁₀ H ₈ BaO ₇ S ₂	C ₁₀ H ₈ BaO ₇ S ₂	C ₁₀ H ₁₀ BaO ₈ S ₂
Formula weight	441.62	441.62	459.64
Temperature	293(2)	293(2)	293(2)
Wavelength (Å) /MoK _α	0.71073	0.71073	0.71073
Crystal system	orthorhombic	orthorhombic	orthorhombic
Space group	<i>Pnma</i>	<i>Pbca</i>	<i>Pna2₁</i>
<i>a</i> (Å)	9.8122(13)	10.0434(11)	13.269(3)
<i>b</i> (Å)	22.140(3)	11.1624(9)	19.337(5)
<i>c</i> (Å)	6.0060(8)	22.5016(15)	5.3625(12)
α (°)	90	90	90
β (°)	90	90	90
γ (°)	90	90	90
<i>V</i> (Å ³)	1304.7(3)	2522.6(4)	1375.9(6)
<i>Z</i>	4	8	4
<i>Calcd.</i> density (g cm ⁻³)	2.248	2.326	2.219
Absorption coefficient (mm ⁻¹)	3.391	3.508	3.226
<i>F</i> (000)	848	1696	888
2 θ range	7.956 to 54.966	7.244 to 54.996	7.028 to 54.996
Reflections collected	8275	17456	13774
Completeness to $\theta = 27.49^\circ$	98.2%	98.9%	99.0%
Data/restraints/parameters	1506/0/99	2862/0/190	3107/1/195
Goodness-of-fit on <i>F</i> ²	1.087	1.058	1.074
Final <i>R</i> indices [<i>I</i> > 2 σ (<i>I</i>)]	<i>R</i> ₁ = 0.0175 <i>wR</i> ₂ = 0.0416	<i>R</i> ₁ = 0.0221 <i>wR</i> ₂ = 0.0482	<i>R</i> ₁ = 0.0136 <i>wR</i> ₂ = 0.0347

^a*R*₁ = $\sum(F_o - F_c)/\sum F_o$. ^b*wR*₂ = $[\sum w(F_o^2 - F_c^2)^2/\sum w(F_o^2)^2]^{1/2}$.

Table S2. Selected bond lengths (Å) and bond angles (°) in compounds **1-3**.

Compound 1			
Ba(1)–O(1)	2.6801(18)	Ba(1)–O(2)#4	2.7030(18)
Ba(1)–O(3)#1	2.7344(18)	Ba(1)–O(1W)#5	3.104(3)
Ba(1)–O(3)#2	2.7344(18)	Ba(1)–O(1W)	2.892(3)
Ba(1)–O(2)#3	2.7030(18)	Ba(1)–O(1)#6	2.6801(18)
O(3)#1–Ba(1)–O(3)#2	79.40(9)	O(1W)–Ba(1)–O(1W)#3	134.65(5)
O(3)#1–Ba(1)–O(1W)#3	131.48(5)	O(1)#6–Ba(1)–O(3)#2	68.49(7)
O(3)#1–Ba(1)–O(1W)	79.23(7)	O(1)#6–Ba(1)–O(3)#1	111.66(7)
O(3)#2–Ba(1)–O(1W)#3	131.48(5)	O(1)–Ba(1)–O(3)#2	111.66(7)
O(3)#2–Ba(1)–O(1W)	79.23(7)	O(1)–Ba(1)–O(3)#1	68.49(7)
O(2)#4–Ba(1)–O(3)#2	88.58(7)	O(1)#6–Ba(1)–O(2)#5	138.36(8)
O(2)#5–Ba(1)–O(3)#2	153.08(7)	O(1)–Ba(1)–O(2)#4	138.36(8)
O(2)#5–Ba(1)–O(3)#1	88.58(7)	O(1)#6–Ba(1)–O(2)#4	85.48(7)
O(2)#4–Ba(1)–O(3)#1	153.08(7)	O(1)–Ba(1)–O(2)#5	85.48(7)
O(2)#4–Ba(1)–O(2)#5	91.66(9)	O(1)#6–Ba(1)–O(1W)#3	65.33(7)
O(2)#5–Ba(1)–O(1W)#3	73.96(6)	O(1)#6–Ba(1)–O(1W)	142.51(5)
O(2)#4–Ba(1)–O(1W)#3	73.96(6)	O(1)–Ba(1)–O(1W)#3	65.33(7)
O(2)#5–Ba(1)–O(1W)	74.88(7)	O(1)–Ba(1)–O(1W)	142.51(5)
O(2)#4–Ba(1)–O(1W)	74.88(7)	O(1)#6–Ba(1)–O(1)	70.32(8)
Compound 2			
Ba(1)–O(5)#1	2.802(2)	Ba(1)–O(2)#5	2.805(2)
Ba(1)–O(4)#2	2.716(2)	Ba(1)–O(1)	2.691(2)
Ba(1)–O(3)#3	2.810(2)	Ba(1)–O(1W)#6	3.267(3)
Ba(1)–O(6)#4	2.816(2)	Ba(1)–O(1W)	2.809(3)
Ba(1)–O(6)#1	3.320(3)		

O(5)#1–Ba(1)–O(3)#2	78.02(7)	O(2)#4–Ba(1)–O(3)#2	138.40(9)
O(5)#1–Ba(1)–O(6)#1	44.76(6)	O(2)#4–Ba(1)–O(6)#3	92.30(7)
O(5)#1–Ba(1)–O(6)#3	135.63(8)	O(2)#4–Ba(1)–O(6)#1	64.96(7)
O(5)#1–Ba(1)–O(2)#4	83.87(7)	O(2)#4–Ba(1)–O(1W)	66.30(8)
O(5)#1–Ba(1)–O(1W)	76.06(8)	O(2)#4–Ba(1)–O(1W)#5	83.58(7)
O(5)#1–Ba(1)–O(1W)#5	92.99(7)	O(1)–Ba(1)–O(5)#1	153.42(9)
O(4)#6–Ba(1)–O(5)#1	84.39(7)	O(1)–Ba(1)–O(4)#6	81.13(7)
O(4)#6–Ba(1)–O(3)#2	75.54(8)	O(1)–Ba(1)–O(3)#2	119.14(9)
O(4)#6–Ba(1)–O(6)#1	79.72(7)	O(1)–Ba(1)–O(6)#3	70.73(10)
O(4)#6–Ba(1)–O(6)#3	122.19(8)	O(1)–Ba(1)–O(6)#1	110.30(9)
O(4)#6–Ba(1)–O(2)#4	139.62(8)	O(1)–Ba(1)–O(2)#4	92.87(8)
O(4)#6–Ba(1)–O(1W)	145.74(8)	O(1)–Ba(1)–O(1W)	126.58(9)
O(4)#6–Ba(1)–O(1W)#5	58.64(7)	O(1)–Ba(1)–O(1W)#5	60.44(10)
O(3)#2–Ba(1)–O(6)#1	119.25(6)	O(1W)–Ba(1)–O(3)#2	73.07(9)
O(3)#2–Ba(1)–O(6)#3	76.06(7)	O(1W)–Ba(1)–O(6)#3	62.24(9)
O(3)#2–Ba(1)–O(1W)	134.03(8)	O(1W)#5–Ba(1)–O(6)#1	52.37(7)
O(6)#3–Ba(1)–O(6)#1	157.190(15)	O(1W)–Ba(1)–O(6)#1	104.07(8)
O(6)#3–Ba(1)–O(1W)	130.62(8)	O(1W)–Ba(1)–O(1W)#5	148.67(6)
Compound 3			
Ba(1)–O(1)	2.652(2)	Ba(1)–O(4)#4	2.700(2)
Ba(1)–O(3)#1	2.787(2)	Ba(1)–O(2W)#3	3.029(4)
Ba(1)–O(6)#2	2.727(3)	Ba(1)–O(2W)	2.893(4)
Ba(1)–O(2)#3	2.796(2)	Ba(1)–O(1W)	2.802(2)
O(1)–Ba(1)–O(3)#1	105.84(7)	O(2)#3–Ba(1)–O(2W)	128.44(6)
O(1)–Ba(1)–O(6)#3	99.87(8)	O(2)#3–Ba(1)–O(2W)#3	64.03(7)
O(1)–Ba(1)–O(2)#3	76.16(7)	O(2)#3–Ba(1)–O(1W)	137.37(9)
O(1)–Ba(1)–O(4)#4	75.31(8)	O(4)#4–Ba(1)–O(3)#1	147.83(8)

O(1)–Ba(1)–O(2W)	73.50(7)	O(4)#4–Ba(1)–O(6)#2	72.42(8)
O(1)–Ba(1)–O(2W)#3	140.07(7)	O(4)#4–Ba(1)–O(2)#3	134.93(7)
O(1)–Ba(1)–O(1W)	143.58(11)	O(4)#4–Ba(1)–O(2W)#3	136.72(7)
O(3)#1–Ba(1)–O(2)#3	74.02(6)	O(4)#4–Ba(1)–O(2W)	74.15(8)
O(3)#1–Ba(1)–O(2W)	75.49(7)	O(4)#4–Ba(1)–O(1W)	82.69(8)
O(3)#1–Ba(1)–O(2W)#3	61.38(7)	O(2W)–Ba(1)–O(2W)#3	129.77(7)
O(3)#1–Ba(1)–O(1W)	78.40(7)	O(1W)–Ba(1)–O(2W)	72.75(10)
O(6)#2–Ba(1)–O(3)#1	136.54(8)	O(1W)–Ba(1)–O(2W)#3	74.39(10)
O(6)#2–Ba(1)–O(2)#3	79.01(7)		
O(6)#2–Ba(1)–O(2W)	146.49(7)		
O(6)#2–Ba(1)–O(2W)#3	76.36(8)		
O(6)#2–Ba(1)–O(1W)	100.66(9)		

Symmetric codes:

For compound **1**: #1 $-1/2 + x, 3/2 - y, 1/2 - z$; #2 $-1/2 + x, y, 1/2 - z$; #3 $x, y, 1 + z$; #4 $x, 3/2 - y, 1 + z$; #5 $1/2 + x, y, 3/2 - z$; #6 $x, 3/2 - y, z$; #7 $1 - x, 1 - y, -z$.

For compound **2**: #1 $x, 1/2 - y, -1/2 + z$; #2 $1/2 - x, 1 - y, -1/2 + z$; #3 $1 - x, 1 - y, 1 - z$; #4 $1/2 + x, y, 3/2 - z$; #5 $1/2 - x, -1/2 + y, z$; #6 $-1/2 + x, 1/2 - y, 1 - z$.

For compound **3**: #1 $2 - x, 1 - y, 1/2 + z$; #2 $1/2 + x, 1/2 - y, 1 + z$; #3 $x, y, 1 + z$; #4 $1/2 + x, 1/2 - y, z$.

Table S3. Hydrogen bonds information within compounds **1** and **3**.

Compound 1					
D–H	A	d(D–H) (Å)	d(H...A) (Å)	∠DHA (°)	d(D...A) (Å)
O1W–H1W	O3[ARU] ¹	0.863	2.621	144.60	3.362
Compound 3					
O1W–	O5[ARU] ²	0.893	2.041	164.19	2.911

Translation of ARU-Code to CIF and Equivalent Position Code:

$$[\text{ARU}]^1 = -1/2 + x, 3/2 - y, 3/2 - z; [\text{ARU}]^2 = x + 1, y, z.$$

Table S4 Calculation results of the effective atomic number (Z_{eff}) values of compounds **1-3** as well as some commercially used scintillators.⁹

	Molecular formula	Component	Z_{eff}
1	[Ba(1,5-nds)H ₂ O] _n	C ₁₀ H ₈ BaO ₇ S ₂	41.86
2	[Ba(1,6-nds)H ₂ O] _n	C ₁₀ H ₈ BaO ₇ S ₂	41.86
3	[Ba(2,7-nds)(H ₂ O) ₂] _n	C ₁₀ H ₁₀ BaO ₈ S ₂	41.44
Inorganic	BaF ₂	BaF ₂	52.7
	CsF	CsF	53.2
	LaBr ₃	LaBr ₃ :Ce ³⁺	46.9
	PWO	PbWO ₄	75.6
	BGO	Bi ₄ Ge ₃ O ₁₂	75.2
	ZnS	ZnS:Ag ⁺	27.4
	Organic	Anthracene	C ₁₄ H ₁₀
Naphthalene		C ₁₀ H ₈	5.18

Notes: In the approximation of dominance of photoelectric effect for X-rays and of the atomic mass in proportion to the atomic number Z , the Z_{eff} value for a compound A_xB_yC_z can be given by the following equation:¹⁰

$$Z_{\text{eff}} = [(xM_a Z_a^4 + yM_b Z_b^4 + zM_c Z_c^4)/(xM_a + yM_b + zM_c)]^{1/4}$$

where M_a , M_b and M_c are the atomic masses of A, B and C, respectively; Z_a , Z_b and Z_c are atomic numbers of A, B and C, respectively.

Determination of the Z_{eff} value for compound **1** (C₁₀H₈BaO₇S₂):

$$Z_{\text{eff}} = [(10 \times 12.01 \times 6^4 + 8 \times 1.008 \times 1^4 + 1 \times 137.327 \times 56^4 + 7 \times 16.00 \times 8^4 + 2 \times 32.06 \times 16^4)/(10 \times 12.01 + 8 \times 1.008 + 1 \times 137.327 + 7 \times 16.00 + 2 \times 32.06)]^{1/4} = 41.86;$$

Determination of the Z_{eff} value for compound **2** (C₁₀H₈BaO₇S₂):

$$Z_{\text{eff}} = [(10 \times 12.01 \times 6^4 + 8 \times 1.008 \times 1^4 + 1 \times 137.327 \times 56^4 + 7 \times 16.00 \times 8^4 +$$

$$2 \times 32.06 \times 16^4) / (10 \times 12.01 + 8 \times 1.008 + 1 \times 137.327 + 7 \times 16.00 + 2 \times 32.06)]^{1/4} = 41.86;$$

Determination of the Z_{eff} value for compound **3** ($C_{10}H_{10}BaO_8S_2$):

$$Z_{eff} = [(10 \times 12.01 \times 6^4 + 10 \times 1.008 \times 1^4 + 1 \times 137.327 \times 56^4 + 8 \times 16.00 \times 8^4 + 2 \times 32.06 \times 16^4) / (10 \times 12.01 + 10 \times 1.008 + 1 \times 137.327 + 8 \times 16.00 + 2 \times 32.06)]^{1/4} = 41.44.$$

References

1. CrysAlisPro, Agilent Technologies, Version 1.171.37.33, 2014.
2. O.-V. Dolomanov, L.-J. Bourhis, R.-J. Gildea, J.-A.K. Howard and H. Puschmann, *J. Appl. Cryst.* **2009**, *42*, 339–341.
3. G.M. Sheldrick, *Acta Cryst. A*, **2015**, *71*, 3–8.
4. A. L. Spek, *J. Appl. Cryst.* **2003**, *36*, 7–13.
5. J. Lu, X.-H. Xin, Y.-J. Lin, S.-H. Wang, J.-G. Xu, F.-K. Zheng and G.-C. Guo, *Dalton Trans.*, **2019**, *48*, 1722–1731.
6. M. C. Payne, M. P. Teter, D. C. Allan, T. A. Arias, J. D. Joannopoulos, *Rev. Mod. Phys.* **1992**, *64*, 1045–1097.
7. X.-L. Zhang, G.-M. Tang, Y.-T. Wang, *Polyhedron*, **2018**, *148*, 55–69.
8. V. Balzani, P. Ceroni, A. Juris. *Photochemistry and photophysics: concepts, research, applications*, Wiley, **2014**.
9. F. Maddalena, L. Tjahjana, A. Xie, Arramel, S. Zeng, H. Wang, P. Coquet, W. Drozdowski, C. Dujardin, C. Dang and M. Birowosuto, *Crystals*, **2019**, *9*, 88.
10. J. Lu, S.-H. Wang, Y. Li, W. F. Wang, C. Sun, P.-X. Li, F.-K. Zheng and G.-C. Guo, *Dalton Trans.*, **2020**, *49*, 7309–7314.